

# Knowledge-and-Data-Driven Amplitude Spectrum Prediction for Hierarchical Neural Vocoders

Yang Ai, Zhen-Hua Ling

National Engineering Laboratory for Speech and Language Information Processing  
University of Science and Technology of China, Hefei, P.R.China

ay8067@mail.ustc.edu.cn, zhling@ustc.edu.cn

## Abstract

In our previous work, we have proposed a neural vocoder called HiNet which recovers speech waveforms by predicting amplitude and phase spectra hierarchically from input acoustic features. In HiNet, the amplitude spectrum predictor (ASP) predicts log amplitude spectra (LAS) from input acoustic features. This paper proposes a novel knowledge-and-data-driven ASP (KDD-ASP) to improve the conventional one. First, acoustic features (i.e., F0 and mel-cepstra) pass through a knowledge-driven LAS recovery module to obtain approximate LAS (ALAS). This module is designed based on the combination of STFT and source-filter theory, in which the source part and the filter part are designed based on input F0 and mel-cepstra, respectively. Then, the recovered ALAS are processed by a data-driven LAS refinement module which consists of multiple trainable convolutional layers to get the final LAS. Experimental results show that the HiNet vocoder using KDD-ASP can achieve higher quality of synthetic speech than that using conventional ASP and the WaveRNN vocoder on a text-to-speech (TTS) task.

**Index Terms:** neural vocoder, log amplitude spectrum, source-filter, TTS

## 1. Introduction

Recently, statistical parametric speech synthesis (SPSS) has become a widely used text-to-speech (TTS) framework due to its high quality and flexibility. Both acoustic models which predict acoustic features (e.g., mel-cepstra and F0) from texts and vocoders [1] which reconstruct speech waveforms from predicted acoustic features play important roles in SPSS. Some conventional vocoders, such as STRAIGHT [2] and WORLD [3] which are designed based on the source-filter model of speech production [4], have been popularly applied in current SPSS systems. However, these vocoders still have some deficiencies, such as the loss of spectral details and phase information.

In recent years, some autoregressive neural generative models such as WaveNet [5], SampleRNN [6] and WaveRNN [7] for raw audio signals have been proposed and demonstrated good performance. Subsequently, some variants such as knowledge-distilling-based models (e.g., parallel WaveNet [8] and ClariNet [9]) and flow-based models (e.g., WaveGlow [10]) were also proposed to further improve the performance and efficiency of generation. Neural vocoders based on these waveform generation models [11, 12, 13, 14, 15, 16] have been developed to reconstruct speech waveforms from various acoustic features for SPSS and some other tasks, such

as voice conversion [17, 18], bandwidth extension [19] and speech coding [20]. Experimental results confirmed that these neural vocoders performed significantly better than conventional ones. However, there are still some limitations with current neural vocoders. The autoregressive neural vocoders are very inefficient at synthesis time due to their point-by-point generation process. For knowledge-distilling-based vocoders and flow-based vocoders, it is difficult to train them due to their complicated training process and high complexity of model structures respectively.

Recently, some improved neural vocoders, such as glottal neural vocoder [21, 22], LPCNet [23], and neural source-filter (NSF) vocoder [24, 25, 26, 27], have been further proposed by combining speech production mechanisms with neural networks and have also demonstrated impressive performance. In our previous work [28], we proposed a neural vocoder named HiNet which recovers speech waveforms by predicting amplitude and phase spectra hierarchically from input acoustic features. The HiNet vocoder is composed of an amplitude spectrum predictor (ASP) and a phase spectrum predictor (PSP). The outputs of ASP and PSP are combined to recover speech waveforms by short-time Fourier synthesis (STFS). Besides, generative adversarial networks (GANs) [29] are also introduced into ASP and PSP to further improve the performance of the HiNet vocoder. Experimental results show that the proposed HiNet vocoder can generate waveforms with high quality and high efficiency.

In this paper, we propose a novel knowledge-and-data-driven ASP (KDD-ASP) to replace the conventional one in a HiNet vocoder. The aim of KDD-ASP is to integrate speech production and analysis knowledge into data-driven LAS prediction, expecting to improve the accuracy and generalization ability of ASP, especially when predicted acoustic features are used as input. KDD-ASP consists of a knowledge-driven LAS recovery module and a data-driven LAS refinement module. The first module is designed based on the combination of STFT and the source-filter theory of speech production, and generates approximate LAS (ALAS) from input acoustic features (i.e., F0 and mel-cepstra). We assume that the speech signal is produced via a source-filter process [4]. The source excitation signal and the filter are designed according to the input F0 and mel-cepstra respectively. Then, ALAS can be calculated by imitating the process of STFT which includes truncation, windowing and FFT. All operations are performed in the frequency domain. The second module predicts the final LAS from ALAS. This module consists of multiple trainable convolutional layers and is trained in a data-driven way. Experimental results confirm that the HiNet vocoder using KDD-ASP can achieve higher quality of synthetic speech than that using conventional ASP and the WaveRNN vocoder on a TTS task.

This paper is organized as follows. In Section 2, we briefly

This work was partially funded by the National Natural Science Foundation of China under Grant 61871358.

review the HiNet vocoder [28]. In Section 3, we describe the details of our proposed KDD-ASP. Section 4 reports our experimental results. Conclusions are given in Section 5.

## 2. HiNet vocoder

HiNet [28] is a novel neural vocoder which recovers speech waveforms by predicting amplitude and phase spectra hierarchically from input acoustic features. Different from existing neural vocoders which directly generate waveform samples using single neural networks, the HiNet vocoder is composed of an amplitude spectrum predictor (ASP) and a phase spectrum predictor (PSP). ASP predicts frame-level log amplitude spectra (LAS) from acoustic features. Then, the predicted LAS and F0 are sent into the PSP for phase recovery. Finally, the outputs of ASP and PSP are combined to recover speech waveforms by short-time Fourier synthesis (STFS).

In our implement, ASP is a simple DNN consisting of multiple feed-forward (FF) layers without any autoregressive structures. ASP uses concatenated acoustic features at current frame along with previous frames as input and outputs log amplitude spectra (LAS) at current frame. At the training stage, the target LAS are extracted from natural waveforms by STFT. GANs are also introduced into ASP. ASP is used as the generator and the discriminator consists of multiple convolutional layers which operate along the frequency axis of the input LAS. A Wasserstein GAN [30] loss is used for training the generator together with the mean square error (MSE) between the predicted LAS and natural ones.

PSP is constructed by concatenating a neural waveform generator with a phase extractor. The neural waveform generator is built by adapting the NSF vocoder [24] from three aspects, 1) using LAS as the input, 2) pre-calculating the initial phase of the sine-based excitation signal for each voiced segment at the training stage and 3) adopting a combined loss function including MSE on amplitude spectra, waveform loss and correlation loss. GANs are also introduced into PSP. The neural waveform generator is used as the generator and the discriminator is similar with that of ASP but its input is waveform.

## 3. Knowledge-and-Data-Driven ASP

This paper proposes a novel knowledge-and-data-driven ASP (KDD-ASP) to replace the conventional one in a HiNet vocoder. The KDD-ASP is constructed by concatenating a knowledge-driven LAS recovery module with a data-driven LAS refinement module as shown in Fig. 1.

### 3.1. Knowledge-driven LAS recovery module

The equation for extracting LAS directly from a signal  $s$  by STFT can be written as follows,

$$\mathbf{LAS}_n = \log |\mathcal{F}(s_n \odot \mathbf{w})|, \quad (1)$$

where  $s_n = [s_{n,1}, \dots, s_{n,L}]^\top$  and  $\mathbf{LAS}_n = [\mathbf{LAS}_{n,1}, \dots, \mathbf{LAS}_{n,K}]^\top$  are the framed signal of  $s$  and the LAS at the  $n$ -th frame respectively, and  $\mathbf{w} = [w_1, \dots, w_L]^\top$  denotes the Hanning window for short-time analysis.  $L$  is the frame number.  $K = \frac{FN}{2} + 1$  represents the number of frequency bins and  $FN$  is the FFT point number.  $\odot$  and  $\mathcal{F}$  represent element-wise product and FFT, respectively.

Inspired by this process, the knowledge-driven LAS recovery module constructs approximate LAS (ALAS) from F0 and

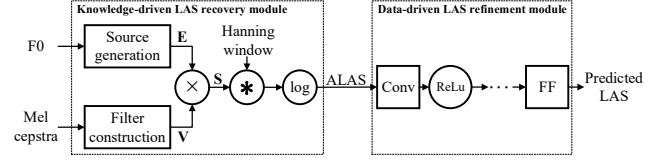


Figure 1: *Model structure of KDD-ASP. Here,  $\times$ ,  $*$  and  $\log$  denote element-wise product, convolutional and log operation respectively, FF and Conv represent feed-forward and convolutional layers respectively and ReLu means rectified linear units.*

mel-cepstra based on the frequency-domain representation of Eq. (1). We assume that the speech signal at the  $n$ -th frame  $s_n$  is obtained by the convolution between a source excitation signal  $e_n$  and a filter impulse response  $v_n$ . In frequency domain, this process can be represented as

$$\mathbf{S}_n = \mathbf{E}_n \odot \mathbf{V}_n, \quad (2)$$

where  $\mathbf{S}_n = [S_{n,1}, \dots, S_{n,K}]^\top$ ,  $\mathbf{E}_n = [E_{n,1}, \dots, E_{n,K}]^\top$  and  $\mathbf{V}_n = [V_{n,1}, \dots, V_{n,K}]^\top$  are the Fourier transform of  $s_n$ ,  $e_n$  and  $v_n$  respectively.

Let  $f_n$  denote the F0 value of the  $n$ -th frame when it is voiced and  $f_n = 0$  when the frame is unvoiced. For voiced frames ( $f_n > 0$ ),  $\mathbf{E}_n$  is produced as a pulse train with equal frequency interval  $K_0 = \text{Round}(\frac{f_n}{F_s} \cdot FN)$ , which corresponds to constructing all the harmonics below the Nyquist frequency, where  $F_s$  is the sampling rate. For unvoiced frames ( $f_n = 0$ ), we set  $E_n \equiv 1$ , meaning that the excitation signal is a Gaussian white noise. The equation for producing  $\mathbf{E}_n$  based on F0 values can be written as

$$E_{n,k} = \begin{cases} 1, & f_n > 0, k = i \cdot K_0 \\ 0, & f_n > 0, k \neq i \cdot K_0 \text{ or } f_n = 0 \end{cases}, \quad (3)$$

where  $i = 1, 2, \dots, \lceil \frac{K}{K_0} \rceil$ .

$\mathbf{V}_n$  is calculated by transforming mel-cepstra to amplitude spectra [31]. The mel-cepstral coefficients at the  $n$ -th frame (with energy as the first order) are first padded with zeros to form a  $K$ -dimensional vector  $\mathbf{m}_n = [m_{n,1}, \dots, m_{n,K}]^\top$ . Then, the cepstral coefficients  $c_{n,k}, k = 1, \dots, K$  are calculated by the following iterative formulas

$$c_{n,k}(i) = \begin{cases} m_{n,i} - \alpha \cdot c_{n,1}(i+1), & k=1 \\ (1-\alpha^2) \cdot c_{n,1}(i+1) - \alpha \cdot c_{n,2}(i+1), & k=2 \\ c_{n,k-1}(i+1) - \alpha \cdot [c_{n,k}(i+1) - c_{n,k-1}(i)], & k>2 \end{cases}, \quad (4)$$

where  $i$  iterates from  $K$  to 1 with the initial value  $c_{n,k}(K+1) = 0, k = 1, \dots, K$ .  $\alpha$  is the mel-frequency warping coefficient, which is 0.42 for  $F_s = 16000$ . After the iteration, we can obtain the cepstra vector  $\mathbf{c}_n = [c_{n,1}(1), \dots, c_{n,K}(1)]^\top$ , which is further transformed to the amplitude spectra  $\mathbf{V}_n$  by

$$\mathbf{V}_n = \exp[\mathcal{F}(\mathbf{c}_n)]. \quad (5)$$

Finally, ALAS can be calculated as

$$\mathbf{ALAS}_n = \log |\mathbf{S}_n * \mathbf{W}|, \quad (6)$$

where  $\mathbf{ALAS}_n = [\mathbf{ALAS}_{n,1}, \dots, \mathbf{ALAS}_{n,K}]^\top$  is the  $n$ -th frame ALAS and  $\mathbf{W} = [W_1, \dots, W_K]^\top$  is the Fourier transform of the analysis window  $w$ . The operation  $*$  represents convolution. It is worth mentioning that the elements in the vectors of  $\mathbf{S}_n$  and  $\mathbf{W}$  should be rearranged by complementing their mirror-symmetric parts and shifting the zero-frequency component to the center before convolution.

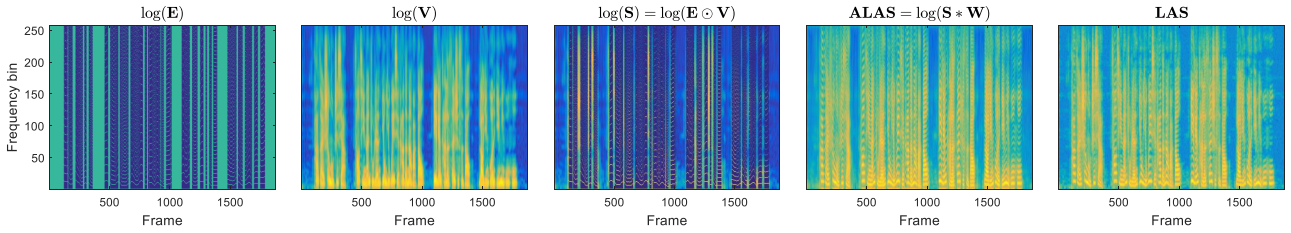


Figure 2: The visualization of  $\log(\mathbf{E}_n)$ ,  $\log(\mathbf{V}_n)$ ,  $\log(\mathbf{S}_n)$ ,  $\mathbf{ALAS}_n$  and  $\mathbf{LAS}_n$  for an example utterance. Here, the input F0 and mel-cepstra are natural ones.

### 3.2. Data-driven LAS refinement module

The data-driven LAS refinement module converts ALAS to final LAS by a trainable neural network. In our implement, this module adopts the ASP model in Section 2 but has two structural improvements. First, convolutional layers are used instead of FF layers in the generator and the input is the ALAS at current frame instead of the concatenated ones as shown in Fig. 1. Second, another discriminator which operates along with the time axis of the input LAS is added<sup>1</sup>.

## 4. Experiments

### 4.1. Experimental conditions

A Chinese speech synthesis corpus with 13334 utterances ( $\sim 20$  hours) from a female speaker was used in our experiments. The waveforms had 16kHz sampling rate and 16bits resolution. We chose 13134 and 100 utterances to construct the training set and validation set respectively, and the remaining 100 utterances were used as the test set. The natural acoustic features were extracted by STRAIGHT and the window size was 25ms and the window shift was 5ms. The acoustic features at each frame were 43-dimensional including 40-dimensional mel-cepstra, an energy, an F0 and a V/UV flag. For TTS, a bidirectional LSTM-RNN acoustic model [32] having 2 hidden layers with 1024 units per layer (512 forward units and 512 backward units) was trained to predict acoustic features from 566-dimensional linguistic features which were divided by natural durations. The output of the acoustic model contained acoustic features together with their delta and acceleration counterparts, which were totally 127 dimensions (the V/UV flag had no dynamic components). Then, the predicted acoustic features were generated from the output by maximum likelihood parameter generation (MLPG) algorithm [33] considering global variance (GV) [34].

Three vocoders were compared in our experiments<sup>2</sup>. The descriptions of these vocoders are as follows.

1) **WaveRNN** A 16-bit WaveRNN-based neural vocoder using acoustic features as input implemented by ourselves. The structure was the same as **WaveRNN** in our previous work [28] which performed better than the 16-bit WaveNet vocoder using open source implementation<sup>3</sup>. The efficiency optimization strategies [7] were not adopted here. The waveform samples were quantized to discrete values by 16-bit linear quantization and the built model had one hidden layer of 1024 nodes where 512 nodes for coarse outputs and another 512 nodes for fine

outputs. Models were trained and evaluated on a single Nvidia 1080Ti GPU using TensorFlow framework [35].

2) **HiNet** A HiNet vocoder using conventional ASP. The structure of ASP is the same with that of the data-driven LAS refinement module introduced in Section 3.2. When extracting natural LAS, the frame length and frame shift of STFT were 20ms (i.e.,  $L = 320$ ) and 5ms respectively and FFT point number was 512 (i.e.,  $K = 257$ ). There were 3 convolutional layers with 2048 nodes per layer (filter width=7), and a 257-dimensional linear output layer which predicted the LAS. For each training step, ASP used 128 frames of acoustic features as input and outputted corresponding 128 frames of LAS. GANs were also used in ASP. Discriminator #1 operated along with the frequency axis and consisted of 6 convolutional layers (filter width=9, stride size=2) and their channels were 16, 32, 64, 128 and 256 respectively. The resulting dimensions per layer, being it frequency bins  $\times$  channels, were  $257 \times 1$ ,  $129 \times 16$ ,  $65 \times 32$ ,  $33 \times 64$ ,  $17 \times 128$  and  $9 \times 256$ . Finally, two FF layers with 256 and 9 nodes respectively were used to map the  $9 \times 256$  convolutional results into a value for loss calculation. Discriminator #2 operated along with the time axis and consisted of 4 convolutional layers (filter width=9, stride size=2) and their channels were 64, 128, 256 and 512 respectively. The resulting dimensions per layer, being it frequency bins  $\times$  channels, were  $128 \times 257$ ,  $64 \times 64$ ,  $32 \times 128$ ,  $16 \times 256$  and  $8 \times 512$ . Finally, two FF layers with 512 and 8 nodes respectively were used to map the  $8 \times 512$  convolutional results into a value for loss calculation. Remaining settings of ASP and all the settings of PSP are the same as the **HiNet-SGAN** vocoder in our previous work [28]. ASP and PSP models were both trained and evaluated on a single Nvidia 1080Ti GPU using TensorFlow framework [35].

3) **HiNet-KDD** A HiNet vocoder using the KDD-ASP proposed in this paper. For KDD-ASP, the knowledge-driven LAS generation module adopted the same settings with that of extracting natural LAS (i.e.,  $L = 320$  and  $K = 257$ ) and the settings of the data-driven LAS refinement module were the same as the ASP of **HiNet**. The settings of PSP and the implementation conditions were all the same as that of **HiNet**. Fig. 2 shows the visualization of  $\mathbf{E}_n$ ,  $\mathbf{V}_n$ ,  $\mathbf{S}_n$ ,  $\mathbf{ALAS}_n$  and  $\mathbf{LAS}_n$  for all frames in an example utterance. We can see that the recovered ALAS is close to the reference LAS with analogous harmonic and formant structures, meaning that the input and output of the data-driven LAS refinement module are similar, expecting to facilitate the model learning and to improve the performance of predicting amplitude spectra.

### 4.2. Objective evaluation

We first compared the performance of these three vocoders using objective evaluations. Five objective metrics used in our

<sup>1</sup>Discriminators are not shown in Fig. 1 for simplification.

<sup>2</sup>Examples of generated speech can be found at <http://home.ustc.edu.cn/~ay8067/Interspeech2020/demo.html>.

<sup>3</sup>[https://github.com/r9y9/wavenet\\_vocoder](https://github.com/r9y9/wavenet_vocoder).

Table 1: Objective evaluation results of **WaveRNN**, **HiNet** and **HiNet-KDD** on the test set. “AS” stands for analysis-synthesis task and “TTS” stands for TTS task.

	<b>WaveRNN</b>	<b>HiNet</b>	<b>HiNet-KDD</b>
SNR(dB)	4.6631	<b>5.2587</b>	5.0152
LAS-RMSE(dB)	4.9623	<b>4.2602</b>	4.5659
AS MCD-V(dB)	1.0702	<b>0.7686</b>	0.8583
F0-RMSE(cent)	13.2365	9.3345	<b>9.0960</b>
V/UV error(%)	4.2515	2.0116	<b>2.0041</b>
MCD-V(dB)	1.0702	1.0939	<b>0.9488</b>
TTS F0-RMSE(cent)	12.4645	7.0877	<b>6.4970</b>
V/UV error(%)	3.5247	<b>1.7983</b>	2.0194

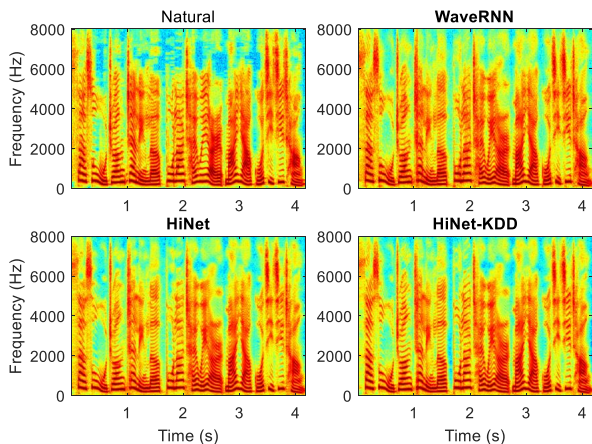


Figure 3: The spectrograms of natural speech and the speech generated by **WaveRNN**, **HiNet** and **HiNet-KDD** on TTS task for an example sentence in the test set.

previous work [28] were adopted here, including signal-to-noise ratio (SNR), root MSE (RMSE) of LAS (denoted by LAS-RMSE), mel-cepstrum distortion for voiced frames (denoted by MCD-V), MSE of F0 (denoted by F0-RMSE) and V/UV error. For the analysis-synthesis (AS) task, the references are natural waveforms or the acoustic features extracted from natural waveforms. For the TTS task, the references are the mel-cepstra and F0 predicted by the acoustic model and only MCD-V, F0-RMSE and V/UV error were adopted since the calculation of SNR and LAS-RMSE relied on natural speech waveforms.

The objective results on the test set are listed in Table 1. It is obvious that both **HiNet** and **HiNet-KDD** outperformed **WaveRNN** on most metrics for both AS and TTS tasks. By comparing **HiNet** and **HiNet-KDD**, we can find that **HiNet-KDD** performed better on F0-RMSE than **HiNet** for both AS and TTS tasks, which indicated that **HiNet-KDD** is better at restoring harmonics for voiced frames. Considering the SNR, LAS-RMSE and MCD-V for AS task, **HiNet-KDD** was not as good as **HiNet**. However, for TTS task, **HiNet-KDD** achieved better MCD-V than **HiNet**. This advantage can be attributed to that using ALAS as the input to train the ASP model improves its generalization ability when dealing with unseen acoustic features. We also draw the spectrograms extracted from natural waveforms and from the waveforms generated by these three vocoders on TTS task in Fig. 3. We can see that **HiNet-KDD** can restore more clear harmonics (e.g., 0.7~1.0s and 1.7~2.0s) especially in the high-frequency band than the other two vocoders.

Table 2: Average preference scores (%) on naturalness among different vocoders, where N/P stands for “no preference” and  $p$  denotes the  $p$ -value of a  $t$ -test between two vocoders. “AS” stands for analysis-synthesis task and “TTS” stands for TTS task.

	<b>WaveRNN</b>	<b>HiNet</b>	<b>HiNet-KDD</b>	N/P	$p$
AS	2.73	<b>72.73</b>	–	24.54	< 0.01
	–	21.36	15.45	63.19	0.15
TTS	16.82	<b>57.27</b>	–	25.91	< 0.01
	10.91	–	<b>66.82</b>	22.27	< 0.01
	–	14.55	<b>53.64</b>	31.81	< 0.01

### 4.3. Subjective evaluation

Five groups of ABX preference tests were conducted to compare the subjective performance of different vocoders. In each subjective test, 20 utterances generated by two comparative vocoders were randomly selected from the test set. Each pair of generated speech were evaluated in random order. 11 Chinese native speakers were asked to be the listeners. The listeners were asked to judge which utterance in each pair had better naturalness or there was no preference. In addition to calculating the average preference scores, the  $p$ -value of a  $t$ -test was used to measure the significance of the difference between two vocoders.

The subjective results are shown in Table 2. We can see that **HiNet** outperformed **WaveRNN** very significantly ( $p < 0.01$ ) on both AS and TTS tasks. However, the preference difference between these two vocoders became weaker on TTS task than on AS task. Comparing **HiNet** with **HiNet-KDD**, we can see that there was no significant difference ( $p > 0.05$ ) between these two vocoders on AS task but **HiNet-KDD** outperformed **HiNet** significantly ( $p < 0.01$ ) on TTS task. We also conducted a group of ABX test between **WaveRNN** and **HiNet-KDD** for TTS task and **HiNet-KDD** also outperformed **HiNet** significantly ( $p < 0.01$ ). Besides, the preference score difference between **HiNet-KDD** and **WaveRNN** was larger than that between **HiNet** and **WaveRNN**. These results all indicated that using KDD-ASP in HiNet vocoder was helpful for improving the quality of reconstructed speech waveforms when the input acoustic features were predicted for TTS.

## 5. Conclusion

In this paper, we have proposed a novel knowledge-and-data-driven amplitude spectrum predictor (KDD-ASP) to replace the conventional one in HiNet, a hierarchical neural vocoder. KDD-ASP consists of a knowledge-driven LAS recovery module and a data-driven LAS refinement module. The first module is designed based on the combination of STFT and source-filter theories in order to convert F0 and mel-cepstra into approximate log amplitude spectra (ALAS). The input F0 values are used to produce the source signal and the filter part is calculated from mel-cepstra. The second module is a convolutional neural network which adopts GANs and predicts the final LAS from input ALAS. Experimental results show that the HiNet vocoder using KDD-ASP can achieve higher quality of synthetic speech than the HiNet vocoder using conventional ASP and the WaveRNN vocoder on a TTS task. To explore other knowledge-driven methods for ASP and further improve the performance of phase spectrum prediction will be the tasks of our future research.

## 6. References

- [1] H. Dudley, "The vocoder," *Bell Labs Record*, vol. 18, no. 4, pp. 122–126, 1939.
- [2] H. Kawahara, I. Masuda-Katsuse, and A. De Cheveigne, "Restructuring speech representations using a pitch-adaptive time-frequency smoothing and an instantaneous-frequency-based f0 extraction: Possible role of a repetitive structure in sounds," *Speech communication*, vol. 27, no. 3, pp. 187–207, 1999.
- [3] M. Morise, F. Yokomori, and K. Ozawa, "WORLD: A vocoder-based high-quality speech synthesis system for real-time applications," *IEICE Transactions on Information and Systems*, vol. 99, no. 7, pp. 1877–1884, 2016.
- [4] F. Gunnar, *The acoustic theory of speech production*. The Hague, The Netherlands: Mouton, 1960.
- [5] A. v. d. Oord, S. Dieleman, H. Zen, K. Simonyan, O. Vinyals, A. Graves, N. Kalchbrenner, A. Senior, and K. Kavukcuoglu, "WaveNet: A generative model for raw audio," in *9th ISCA Speech Synthesis Workshop*, 2016, pp. 125–125.
- [6] S. Mehri, K. Kumar, I. Gulrajani, R. Kumar, S. Jain, J. Sotelo, A. Courville, and Y. Bengio, "SampleRNN: An unconditional end-to-end neural audio generation model," in *Proc. ICLR*, 2017.
- [7] N. Kalchbrenner, E. Elsen, K. Simonyan, S. Noury, N. Casagrande, E. Lockhart, F. Stimberg, A. Oord, S. Dieleman, and K. Kavukcuoglu, "Efficient neural audio synthesis," in *Proc. ICML*, 2018, pp. 2410–2419.
- [8] A. v. d. Oord, Y. Li, I. Babuschkin, K. Simonyan, O. Vinyals, K. Kavukcuoglu, G. v. d. Driessche, E. Lockhart, L. C. Cobo, F. Stimberg *et al.*, "Parallel WaveNet: Fast high-fidelity speech synthesis," in *Proc. ICML*, 2018, pp. 3918–3926.
- [9] W. Ping, K. Peng, and J. Chen, "ClariNet: Parallel wave generation in end-to-end text-to-speech," in *Proc. ICLR*, 2019.
- [10] R. Prenger, R. Valle, and B. Catanzaro, "WaveGlow: A flow-based generative network for speech synthesis," in *Proc. ICASSP*, 2019, pp. 3617–3621.
- [11] A. Tamamori, T. Hayashi, K. Kobayashi, K. Takeda, and T. Toda, "Speaker-dependent WaveNet vocoder," in *Proc. Interspeech*, 2017, pp. 1118–1122.
- [12] T. Hayashi, A. Tamamori, K. Kobayashi, K. Takeda, and T. Toda, "An investigation of multi-speaker training for WaveNet vocoder," in *Proc. ASRU*, 2017, pp. 712–718.
- [13] N. Adiga, V. Tsias, and Y. Stylianou, "On the use of WaveNet as a statistical vocoder," in *Proc. ICASSP*, 2018, pp. 5674–5678.
- [14] Y. Ai, H.-C. Wu, and Z.-H. Ling, "SampleRNN-based neural vocoder for statistical parametric speech synthesis," in *Proc. ICASSP*, 2018, pp. 5659–5663.
- [15] Y. Ai, J.-X. Zhang, L. Chen, and Z.-H. Ling, "DNN-based spectral enhancement for neural waveform generators with low-bit quantization," in *Proc. ICASSP*, 2019, pp. 7025–7029.
- [16] J. Lorenzo-Trueba, T. Drugman, J. Latorre, T. Merritt, B. Putrycz, R. Barra-Chicote, A. Moinet, and V. Aggarwal, "Towards achieving robust universal neural vocoding," in *Proc. Interspeech*, 2019, pp. 181–185.
- [17] L.-J. Liu, Z.-H. Ling, Y. Jiang, M. Zhou, and L.-R. Dai, "WaveNet vocoder with limited training data for voice conversion," in *Proc. Interspeech*, 2018, pp. 1983–1987.
- [18] K. Kobayashi, T. Hayashi, A. Tamamori, and T. Toda, "Statistical voice conversion with WaveNet-based waveform generation," in *Proc. Interspeech*, 2017, pp. 1138–1142.
- [19] Z.-H. Ling, Y. Ai, Y. Gu, and L.-R. Dai, "Waveform modeling and generation using hierarchical recurrent neural networks for speech bandwidth extension," *IEEE/ACM Transactions on Audio, Speech, and Language Processing*, vol. 26, no. 5, pp. 883–894, 2018.
- [20] J. Klejsa, P. Hedelin, C. Zhou, R. Fejgin, and L. Villemoes, "High-quality speech coding with sample RNN," in *Proc. ICASSP*, 2019, pp. 7155–7159.
- [21] Y. Cui, X. Wang, L. He, and F. K. Soong, "A new glottal neural vocoder for speech synthesis," in *Proc. Interspeech*, 2018, pp. 2017–2021.
- [22] L. Juvela, V. Tsias, B. Bollepalli, M. Airaksinen, J. Yamagishi, and P. Alku, "Speaker-independent raw waveform model for glottal excitation," in *Proc. Interspeech*, 2018, pp. 2012–2016.
- [23] J.-M. Valin and J. Skoglund, "LPCNet: Improving neural speech synthesis through linear prediction," in *Proc. ICASSP*, 2019, pp. 5891–5895.
- [24] X. Wang, S. Takaki, and J. Yamagishi, "Neural source-filter-based waveform model for statistical parametric speech synthesis," in *Proc. ICASSP*, 2019, pp. 5916–5920.
- [25] X. Wang and J. Yamagishi, "Neural harmonic-plus-noise waveform model with trainable maximum voice frequency for text-to-speech synthesis," in *Proc. SSW*, 2019, pp. 1–6.
- [26] X. Wang, S. Takaki, and J. Yamagishi, "Neural source-filter waveform models for statistical parametric speech synthesis," *IEEE/ACM Transactions on Audio, Speech, and Language Processing*, vol. 28, pp. 402–415, 2019.
- [27] Y. Zhao, X. Wang, L. Juvela, and J. Yamagishi, "Transferring neural speech waveform synthesizers to musical instrument sounds generation," in *Proc. ICASSP*, 2020, pp. 6269–6273.
- [28] Y. Ai and Z.-H. Ling, "A neural vocoder with hierarchical generation of amplitude and phase spectra for statistical parametric speech synthesis," *IEEE/ACM Transactions on Audio, Speech, and Language Processing*, vol. 28, pp. 839–851, 2020.
- [29] I. Goodfellow, J. Pouget-Abadie, M. Mirza, B. Xu, D. Warde-Farley, S. Ozair, A. Courville, and Y. Bengio, "Generative adversarial nets," in *Advances in neural information processing systems*, 2014, pp. 2672–2680.
- [30] I. Gulrajani, F. Ahmed, M. Arjovsky, V. Dumoulin, and A. C. Courville, "Improved training of Wasserstein GANs," in *Advances in neural information processing systems*, 2017, pp. 5767–5777.
- [31] K. Tokuda, T. Kobayashi, T. Masuko, and S. Imai, "Mel-generalized cepstral analysis—a unified approach to speech spectral estimation," in *Proc. ICSLP*, 1994, pp. 1043–1046.
- [32] Y. Fan, Y. Qian, F.-L. Xie, and F. K. Soong, "TTS synthesis with bidirectional LSTM based recurrent neural networks," in *Proc. Interspeech*, 2014, pp. 1964–1968.
- [33] K. Tokuda, T. Yoshimura, T. Masuko, T. Kobayashi, and T. Kitamura, "Speech parameter generation algorithms for HMM-based speech synthesis," in *Proc. ICASSP*, vol. 3, 2000, pp. 1315–1318.
- [34] T. Toda and K. Tokuda, "A speech parameter generation algorithm considering global variance for HMM-based speech synthesis," *IEICE Transactions on Information and Systems*, vol. 90, no. 5, pp. 816–824, 2007.
- [35] M. Abadi, A. Agarwal, P. Barham, E. Brevdo, Z. Chen, C. Citro, G. S. Corrado, A. Davis, J. Dean, M. Devin *et al.*, "Tensorflow: Large-scale machine learning on heterogeneous distributed systems," 2015. [Online]. Available: <http://download.tensorflow.org/paper/whitepaper2015.pdf>